OXFORD

SOT | Society of Toxicology
www.toxsci.oxfordjournals.org

TOXICOLOGICAL SCIENCES, 169(1), 2019, 280–292

doi: 10.1093/toxsci/kfz038
Advance Access Publication Date: February 14, 2019
Research Article

Cardiac Toxicity From Ethanol Exposure in Human-Induced Pluripotent Stem Cell-Derived Cardiomyocytes

Antonio Rampoldi,[*,1] Monalisa Singh,[*,1] Qingling Wu,[*,†,1] Meixue Duan,[‡] Rajneesh Jha,[*] Joshua T. Maxwell,[*] Joshua M. Bradner,[§] Xiaoyu Zhang,[¶] Anita Saraf,[*,‖] Gary W. Miller,[§] Greg Gibson,[‡] Lou Ann Brown,[*] and Chunhui Xu[*,†,2]

[*]Division of Pediatric Cardiology, Department of Pediatrics, Emory University School of Medicine and Children's Healthcare of Atlanta, Atlanta, Georgia 30322; [†]Wallace H. Coulter Department of Biomedical Engineering, Georgia Institute of Technology and Emory University, Atlanta, Georgia 30332; [‡]School of Biological Sciences, Georgia Institute of Technology, Atlanta, Georgia 30332; [§]Department of Environmental Health, Rollins School of Public Health, Emory University, Atlanta, Georgia 30322; [¶]ACEA Biosciences, Inc., San Diego, California 92121; and [‖]Division of Cardiology, Emory University School of Medicine, Atlanta, Georgia 30322

[1]These authors contributed equally to this study.
[2]To whom correspondence should be addressed at Department of Pediatrics, Emory University School of Medicine, 2015 Uppergate Drive, Atlanta, Georgia 30322. Fax: 404-727-5737; E-mail: chunhui.xu@emory.edu.

ABSTRACT

Alcohol use prior to and during pregnancy remains a significant societal problem and can lead to developmental fetal abnormalities including compromised myocardia function and increased risk for heart disease later in life. Alcohol-induced cardiac toxicity has traditionally been studied in animal-based models. These models have limitations due to physiological differences from human cardiomyocytes (CMs) and are also not suitable for high-throughput screening. We hypothesized that human-induced pluripotent stem cell-derived CMs (hiPSC-CMs) could serve as a useful tool to study alcohol-induced cardiac defects and/or toxicity. In this study, hiPSC-CMs were treated with ethanol at doses corresponding to the clinically relevant levels of alcohol intoxication. hiPSC-CMs exposed to ethanol showed a dose-dependent increase in cellular damage and decrease in cell viability, corresponding to increased production of reactive oxygen species. Furthermore, ethanol exposure also generated dose-dependent increased irregular Ca^{2+} transients and contractility in hiPSC-CMs. RNA-seq analysis showed significant alteration in genes belonging to the potassium voltage-gated channel family or solute carrier family, partially explaining the irregular Ca^{2+} transients and contractility in ethanol-treated hiPSC-CMs. RNA-seq also showed significant upregulation in the expression of genes associated with collagen and extracellular matrix modeling, and downregulation of genes involved in cardiovascular system development and actin filament-based process. These results suggest that hiPSC-CMs can be a novel and physiologically relevant system for the study of alcohol-induced cardiac toxicity.

Key words: cardiomyocytes; calcium handling; ethanol exposure; induced pluripotent stem cells; oxidative stress; RNA-seq.

According to the Center for Disease Control and Prevention, more than 3 million women in the United States are at risk of exposing their fetus to alcohol during early pregnancy (Green *et al.*, 2016). Prenatal alcohol exposure leads to various developmental anomalies including compromised myocardia function (Goh *et al.*, 2011; Kvigne *et al.*, 2004; May *et al.*, 2007; Webster *et al.*, 1984). Heart is the first organ to be established during embryonic development and is highly vulnerable to environmental insults such as alcohol exposure. Impaired heart growth and development in early life can also increase the risk for heart disease later in adulthood (Barker *et al.*, 1989).

© The Author(s) 2019. Published by Oxford University Press on behalf of the Society of Toxicology.
All rights reserved. For permissions, please e-mail: journals.permissions@oup.com

Traditionally, studies on alcohol exposure have relied on animal models and primary cardiomyocytes (CMs) from animals. These studies have established a link between the deleterious effect of ethanol and various cardiac malformations (Piano and Phillips, 2014). However, these models have limitations due to physiological differences from human primary CMs which are difficult to obtain and have limited growth capacity. Indeed, key features of alcohol-related human heart disease including congestive heart failure are not consistently recapitulated in animal models although alcohol decreases cardiac contractility in both animals and human (Fernandez-Sola *et al.*, 2007; Hu *et al.*, 2013). In addition, animal models are not suitable for high-throughput screening in drug discovery. Hence there is an unmet need for developing a physiologically relevant model that can reliably capture and reproduce alcohol-induced heart defects. To complement the studies on animal models/cells and bridge the gap between animal models/cells and human primary CMs, we hypothesized that human-induced pluripotent stem cell-derived CMs (hiPSC-CMs) could serve as a useful tool to study alcohol-induced cardiac defects.

hiPSC-CMs can provide an unlimited supply of physiologically relevant cell source with high-throughput capability for disease modeling and drug discovery. Although there are limitations regarding the use of hiPSC-CMs, these cells express the essential cardiac molecular and functional components that are similar to human primary fetal CMs and can be produced in large quantities (Burridge *et al.*, 2012; Hartman *et al.*, 2016; Laflamme and Murry, 2011; Xu, 2012). These functional hiPSC-CMs have been used as a model to study various cardiac diseases, such as long-QT syndromes (Itzhaki *et al.*, 2011; Jha *et al.*, 2016; Moretti *et al.*, 2010), dilated cardiomyopathy (Sun *et al.*, 2012), catecholaminergic polymorphic ventricular tachycardia (Jung *et al.*, 2012; Kujala *et al.*, 2012; Preininger *et al.*, 2016), and cardiac hypertrophy (Ovchinnikova *et al.*, 2018). In addition, hiPSC-CMs represent a novel tool for the evaluation of cardiac toxicity induced by drugs or other factors (Mercola *et al.*, 2013; Savoji *et al.*, 2019). For example, hiPSC-CMs have been leveraged to examine the toxic effect of cigarettes on heart development (Palpant *et al.*, 2015).

In this study, we explored the possibility of utilizing hiPSC-CMs to examine cardiac phenotypes associated with alcohol exposure. Specifically, we examined the effect of ethanol exposure on cellular, molecular, and functional properties of hiPSC-CMs.

MATERIALS AND METHODS

Generation of hiPSC-CMs by directed differentiation and formation of 3D cardiac spheres. IMR90 hiPSCs (Yu *et al.*, 2007) (by James A. Thomson, University of Wisconsin-Madison, obtained from WiCell Research Institute Inc.) were maintained in a feeder-free condition as described (Xu *et al.*, 2001). Once confluent, cells were induced sequentially with 100 ng/ml activin A on differentiation day 0 and 10 ng/ml BMP4 on differentiation day 1 in RPMI medium containing 2% B27 without insulin (Jha *et al.*, 2016; Preininger *et al.*, 2016). On differentiation day 4, cultures were dissociated using 0.25% trypsin-EDTA, spun for 5 min at 300× g and resuspended for cell counting. Approximately 1750 cells were seeded per microwell in Aggrewell 400 plates (Stem Cell Technologies) cultured in RPMI medium containing 2% B27 and 10 μm Rock inhibitor Y-27632 to facilitate cell survival following dissociation (Nguyen *et al.*, 2014; Watanabe *et al.*, 2007). After 24 h, cardiac spheres were transferred to a suspension culture. Cardiac spheres typically started beating spontaneously by days 10–12 and were cultured until day 20 for subsequent ethanol exposure experiments (Figure 1A).

Rationale for ethanol doses. It is illegal in all jurisdictions within the United States to drive with blood alcohol concentration (BAC) of 0.08% (corresponding to 17 mM ethanol concentration) or more. Blood alcohol concentration higher than 0.2%, 0.3%, and 0.4% progressively corresponds to confusion, stupor and coma leading to alcohol intoxication, respectively. Supplementary Table 1 shows the BAC, corresponding ethanol concentration, and signs and symptoms at that level (adapted from http://www.intox.com/t-physiology.aspx). Several animal studies reported results in response to ethanol exposure with dosages ranging from 25 to 200 mM (Danziger *et al.*, 1991; Delbridge *et al.*, 2000; Mashimo *et al.*, 2003, 2015; Mashimo and Ohno, 2006; Worley *et al.*, 2015). We examined the effects of exposure of hiPSC-CMs to ethanol at the level that was at the legal limit of 17 mM and higher levels that correspond to different levels of alcohol intoxication. Cells were treated with ethanol at 17, 50, 100, and 200 mM in initial experiments. The highest concentration (200 mM) of ethanol had extensive deleterious effects on cell survival and almost all CMs stopped beating at the end of the treatment, hence it was excluded in subsequent experiments.

Immunocytochemical analysis. Cells were dissociated using 0.25% trypsin-EDTA and plated onto a Matrigel-coated 96-well culture plate at a density of 5×10^4 cells/well and cultured for 2 days before fixation. On the day of the immunocytochemical staining, cells were washed with D-PBS and fixed in 2% (vol/vol) paraformaldehyde (Sigma) at room temperature for 15 min and permeabilized in cold methanol for 2 min at room temperature. The cells were then blocked with 5% normal goat serum (NGS) in D-PBS at room temperature for 1–2 h and incubated with the primary antibodies (Supplementary Table 2), including α-actinin (1:800), pan cadherin (1:200), NKX2-5 (1:200), cardiac troponin T (1:400), or cardiac troponin I (1:200) in 1% NGS overnight at 4°C. After the incubation with the primary antibodies, the cells were washed 3 times with D-PBS for 5 min each with gentle agitation to get rid of the unbound primary antibodies. The cells were then incubated with the corresponding conjugated secondary antibodies (1:1000) at room temperature for 1 h in the dark, followed by 3 times wash with D-PBS. The nuclei were counterstained with Vectashield mounting medium containing DAPI (Vector Laboratories, no. H-1200) (Jha *et al.*, 2016; Preininger *et al.*, 2016). Imaging was performed using an inverted microscope (Axio Vert.A1).

xCELLigence-real-time cellular analysis. Impedance-based cell viability and beating activity of hiPSC-CMs were monitored using xCELLigence-real-time cellular analysis (RTCA) CardioECR system (ACEA Biosciences, Inc.). E-Plate Cardio ECR48 (ACEA Biosciences, Inc.) was coated with 100 μl/well of 1:100 fibronectin in DPBS at 37°C for 2 h. After recording baseline reading in RPMI with 2% B27, hiPSC-CMs were dissociated with 0.25% trypsin-EDTA and seeded onto the E-Plate at a density of 6×10^4 cells/well and cultured for 48 h in incubator. Cells were treated with ethanol at final concentrations of 50, 100, and 200 mM for 5 days. Mineral oil was added in treated as well as control wells to prevent ethanol evaporation. RTCA recordings were performed before the ethanol treatment at day 0 and thereafter daily from 1 to 5 days after the ethanol treatment. Data were analyzed using xCELLigence software (ACEA Biosciences, Inc.).

Cell viability and cytotoxicity assay. Cardiac spheres were dissociated using 0.25% trypsin-EDTA and plated onto a Matrigel-

coated 96-well culture plate at a density of 5 $\times 10^4$ cells/well and cultured for 2 days to recover spontaneous beating. Treatment groups were maintained in ethanol-containing medium for 5 days and the medium was covered with mineral oil to prevent ethanol evaporation. On day 5, ethanol-containing medium and mineral oil were aspirated and cells were washed 2 times with warm D-PBS and incubated with 0.5 μM calcein-AM (which labels live cells) and 1 μM ethidium homodimer-1 (which labels dead cells) for 30 min at 37°C in the dark. After the incubation, cells were washed 2 times with warm D-PBS and resuspended in warm phenol red free RPMI containing 2% B27 and immediately proceeded with imaging using an inverted microscope (Axio Vert.A1).

Detection of intracellular reactive oxygen species. Cardiac spheres were dissociated using 0.25% trypsin-EDTA and plated onto a Matrigel-coated 96-well culture plate at a density of 5×10^4 cells/well and cultured for 2 days to recover spontaneous beating. Treatment groups were maintained in ethanol-containing medium which was covered with mineral oil to prevent ethanol evaporation for 5 days. On day 5, ethanol-containing medium and mineral oil were aspirated and cells were washed 2 times with warm D-PBS and incubated with 25 μm carboxy-H2DCFDA (ThermoFisher Scientific) working solution in warm HBSS/Ca^{2+}/Mg^{2+} for 30 min at 37°C, protected from light. Cells were washed 3 times with warm HBSS/Ca^{2+}/Mg^{2+} and counter-stained with Hoechst in warm buffer and imaged immediately using Axio Vert.A1 inverted microscope (Zeiss).

Detection of mitochondrial superoxide production. Cardiac spheres were dissociated using 0.25% trypsin-EDTA and plated onto a Matrigel-coated 96-well culture plate at a density of 5×10^4 cells/well and cultured for 2 days to recover spontaneous beating. Treatment groups were maintained in ethanol-containing medium which was covered with mineral oil to prevent ethanol evaporation for additional 5 days. After the ethanol treatment, ethanol-containing medium and mineral oil were aspirated and cells were washed 2 times with HBSS/Ca^{2+}/Mg^{2+}. The generation of mitochondrial superoxide was assessed using MitoSOX Red (ThermoFisher Scientific). Cells were incubated with 5 μM MitoSOX Red working solution in warm HBSS/Ca^{2+}/Mg^{2+} for 10 min at 37°C, protected from light. Cells were washed 2 times with warm HBSS/Ca^{2+}/Mg^{2+} and counter-stained with Hoechst (ThermoFisher Scientific) in warm buffer and imaged immediately using an ArrayScan XTI Live High Content Platform (Life Technologies).

Images of MitoSOX Red and Hoechst were acquired and quantitatively analyzed using ArrayScan XTI Live High Content Platform. Twenty fields/well were selected and 5 replicate wells per condition were imaged using a 10× objective. Acquisition software Cellomics Scan (ThermoFisher Scientific) was used to capture images, and data analysis was performed using Cellomics View Software (ThermoFisher Scientific). Images were analyzed with mask modifier for Hoechst restricted to the nucleus. MitoSOX Red was quantified with a spot mask that extended 7 units from the nucleus. Spot threshold was set to 10 units and detection limit was set at 25 units. Mean MitoSOX Red average fluorescent fluorescence intensity of cells per well and percentage of MitoSOX Red-positive cells in each treatment group were used as readout.

qRT-PCR (real-time quantitative reverse transcription polymerase chain reaction). RNA was isolated from control and treatment groups ($n = 3$/group) using Aurum total RNA mini kit (Bio-Rad) as per the manufacturer's instructions. Briefly, cells were lysed in 350 μl lysis buffer supplemented with 1% β-mercaptoethanol, and stored at −80°C until further processing. Upon collecting RNA, samples were reverse-transcribed using 100 U of Superscript III enzyme and random primers in 20 μl reaction mixture containing Vilo reaction buffer as per the manufacturer's instructions (SuperScript VILO cDNA Synthesis Kit by Life Technologies). cDNA was further processed in a Bio-Rad thermal cycler upon incubation with the reaction mixture at following temperature cycles: 25°C for 10 min, 42°C for 2 h, and 25°C for 5 min. The reaction mixture was then diluted 15–20 times before further use for real-time PCR (qPCR). Human-specific PCR primers (Supplementary Table 3) for the genes examined were retrieved from Jha *et al*., 2016 and an open access website (http://pga.mgh.harvard.edu/primerbank/). Thermocycler reaction was set up as follows using the iTaq SyBr green master mix: Initial denaturation step at 95°C for 10 min, 40 cycles of 2 steps with 15 s of denaturation at 95°C followed by 1 min of annealing at 60°C using Applied Biosystems 7500 real-time PCR systems. All samples were normalized to the level of the housekeeping gene GAPDH. Relative expression levels compared with control samples were presented as fold changes calculated by the $2^{-\Delta\Delta Ct}$ method. Data are presented as mean ±SD. Statistical significance was analyzed using paired T-test; p values $<.05$ were considered significant.

Cell purity assay. Cardiac spheres were dissociated using 0.25% trypsin-EDTA and plated onto a Matrigel-coated 96-well culture plate at a density of 5×10^4 cells/well and cultured for 2 days to recover spontaneous beating. Treatment groups were maintained in ethanol-containing medium for 5 days and the medium was covered with mineral oil to prevent ethanol evaporation. On day 5, ethanol-containing medium and mineral oil were aspirated and cells were washed with D-PBS and fixed in paraformaldehyde (Sigma) and permeabilized in cold methanol. The cells were then blocked with 5% NGS in D-PBS at room temperature for 1 h and incubated with the primary antibody for NKX2-5 overnight at 4°C. After the incubation with the primary antibody, the cells were washed 3 times with D-PBS and incubated with the corresponding conjugated secondary antibodies followed by 3 times wash with D-PBS. The nuclei were counterstained with Hoechst in warm buffer and imaged using an ArrayScan XTI Live High Content Platform (Life Technologies).

Images of NKX2-5 positive cells and Hoechst were acquired and quantitatively analyzed using ArrayScan XTI Live High Content Platform. Twenty fields/well were selected and 5 replicate wells per condition were imaged using a 10× objective. Acquisition software Cellomics Scan (ThermoFisher Scientific) was used to capture images, and data analysis was performed using Cellomics View Software (ThermoFisher Scientific). Images were analyzed with mask modifier for Hoechst and NKX2-5-positive cells restricted to the nucleus. Percentage of NKX2-5-positive cells and mean average fluorescence intensity of NKX2-5 in each treatment were used as readout.

Calcium imaging. Human-induced pluripotent stem cell-derived CMs were dissociated with 0.05% trypsin-EDTA, seeded onto Matrigel-coated 25× 25 mm glass coverslips and cultured for 2–3 days until they recovered beating. The cells were then treated with 0, 17, and 50 mM of ethanol for 5 days in sealed chambers to prevent ethanol evaporation (Polikandriotis *et al*., 2005). For live cell imaging of intracellular Ca^{2+}, the cells were incubated with 10 μM of Fluo-4 AM (ThermoFisher Scientific) for 30 min at 37°C in culture medium, washed for 30 min, and then

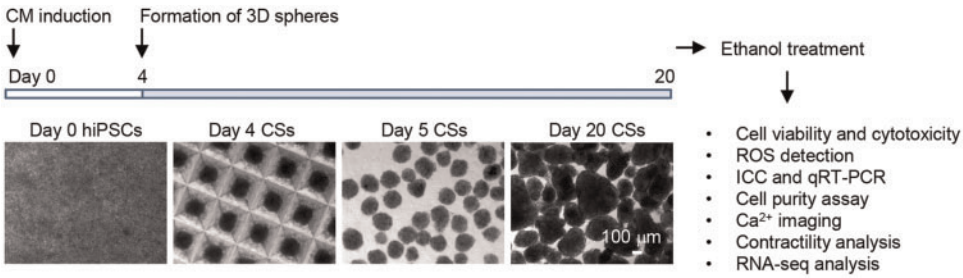

Figure 1. Directed differentiation of hiPSCs and 3D culture of cardiac spheres generate enriched CMs and schematic diagram showing the experimental design. Human-induced pluripotent stem cell-derived cardiomyocytes were directed for CM differentiation and cardiac progenitors were forced to aggregate into 3D cardiac spheres (CSs) at differentiation day 4. Cardiac spheres were subsequently cultured in suspension and monitored for their spontaneous beating activities. Cells at day 20 were used for ethanol exposure and subsequent assessments. ROS, reactive oxygen species; ICC, immunocytochemical analysis; qRT-PCR, real-time quantitative reverse transcription polymerase chain reaction.

transferred to an inverted laser confocal microscope (Olympus FV1000) equipped with FluoView software (Olympus), where they were perfused with normal tyrode solution (140 mM NaCl, 4 mM KCl, 2 mM $CaCl_2$, 1 mM $MgCl_2$, 10 mM HEPES, 5 mM glucose, pH 7.4 with NaOH) (Lian *et al.*, 2012). Fluo-4 was excited by the 488 nm laser and emitted fluorescence was captured at >505 nm. Recordings of Fluo-4 fluorescence were acquired in line-scan mode. Regions exhibiting heterogeneous fluorescence of Fluo-4 were avoided, so as to exclude artifacts (eg, endoplasmic reticulum, mitochondria, vesicles, etc.). Data were analyzed with ClampFit 10.0 software (Molecular Devices) (Burridge *et al.*, 2014).

Video-based analyses of contractility. Contractility of hiPSC-CMs was recorded using a phase contrast inverted microscope (Axio Vert.A1) equipped with Zeiss AxioCam digital camera system, 20× magnification, 30 s for each sample, 100 ms interval between frames. Videos were processed and exported using Zeiss AxioVision LE imaging software. Video-based analysis of contractility parameters was performed with Matlab R2016b software as described (Huebsch *et al.*, 2015).

RNA-seq analysis. RNA was isolated from control and ethanol-treated hiPSC-CMs (n = 3/group) using Aurum total RNA mini kit (Bio-Rad) as per the manufacturer's instructions. RNA concentration was measured using a NanoDrop ND-1000 spectrophotometer (ThermoFisher Scientific). At the high-throughput DNA Sequencing Core, Parker H. Petit Institute for Bioengineering and Bioscience of Georgia Tech, total RNA quality was tested using a 2100 Bioanalyzer, and RNA 6000 Nano Chip (Agilent Technologies) and all samples had RNA integrity number ≥9.4. The Illumina TruSeq technology was then used to prepare RNA-Seq libraries, and next-generation sequencing was done through an Illumina HiSeq 2500, 75 bp paired end sequencing. RNA sequence reads were aligned to the human reference genome (GRCh38) (Kent *et al.*, 2002) using HISAT2 (Kim *et al.*, 2015), followed by using UCSC reference annotation and HTSeq (Anders *et al.*, 2015) to estimate gene abundance. In total, there were 26 485 genes detected, though only 17 671 genes with greater than 5 reads in at least 3 samples were retained for downstream analyses. All downstream analyses were carried out in R v3.4.0 (R Development Core Team, 2014). The DESeq2 R package was used for normalization and detection of differentially expressed genes (Anders and Huber, 2010; Love *et al.*, 2014). The up- and downregulated genes in ethanol-treated samples were identified following Benjamini-Hochberg corrected *p*-value at a significance threshold of .05 (Benjamini and Hochberg, 1995). Functional analysis of the up-/downregulated differentially expressed genes was completed using the ToppFun software package (Chen *et al.*, 2009). Visualization was performed for upregulated gene ontology (GO) terms with FDR values of less than 0.05 and downregulated GO terms with FDR values of less than 0.01.

RESULTS

Directed Differentiation of hiPSCs and 3D Culture Generate Highly Enriched CMs

To generate hiPSC-CMs, we treated hiPSCs sequentially with growth factors activin A and BMP4 at differentiation days 0 and 1, respectively, and then generated cardiac spheres through microscale tissue engineering at day 4 (Figure 1). After suspension culture of the spheres for additional 16 days, cells were characterized for the expression of CM markers by immunocytochemical analysis. As shown in Supplementary Figure 1, the majority of the cells were positive for cardiac transcription factor NKX2-5 and structural proteins including cardiac troponin I, cardiac troponin T and cadherin, suggesting that the 3D cultures contained enriched CMs. These cells were then used for ethanol treatment and subsequent cellular, molecular, and functional assessments.

Ethanol Exposure of hiPSC-CMs Reduces Cell Viability

To examine the effect of ethanol exposure on the survival of hiPSC-CMs, we treated hiPSC-CMs with ethanol at doses corresponding to different levels of alcohol intoxication observed in clinic. We first monitored cellular impedance continuously for over a period of 5 days after the ethanol treatment using xCELLigence-RTCA system. The impedance of electron flow caused by adherent cells was measured noninvasively using microelectrode biosensors and then converted into a parameter called cell index which is positively correlated to the cell number, cell size and morphology, and the quality of cell-substrate attachment. After 3 days, the cell index in untreated group was 86.4% compared with initially seeded cells, whereas the cell index in the 50, 100, and 200 mM ethanol-treated groups decreased to 61.4%, 58.2%, and 3.6%, respectively (Figs. 2A and B). By day 5, the cell index was almost 0 in the group treated with 200 mM ethanol. These results indicate a progressive cell loss in hiPSC-CMs upon ethanol treatment.

Next, we examined cell viability by the LIVE/DEAD staining (which segregates live or calcein-AM positive from dead or ethidium homodimer-1 positive cells) in cultures after 5 days of the treatment with ethanol at 0, 17, 50, 100, and 200 mM. As

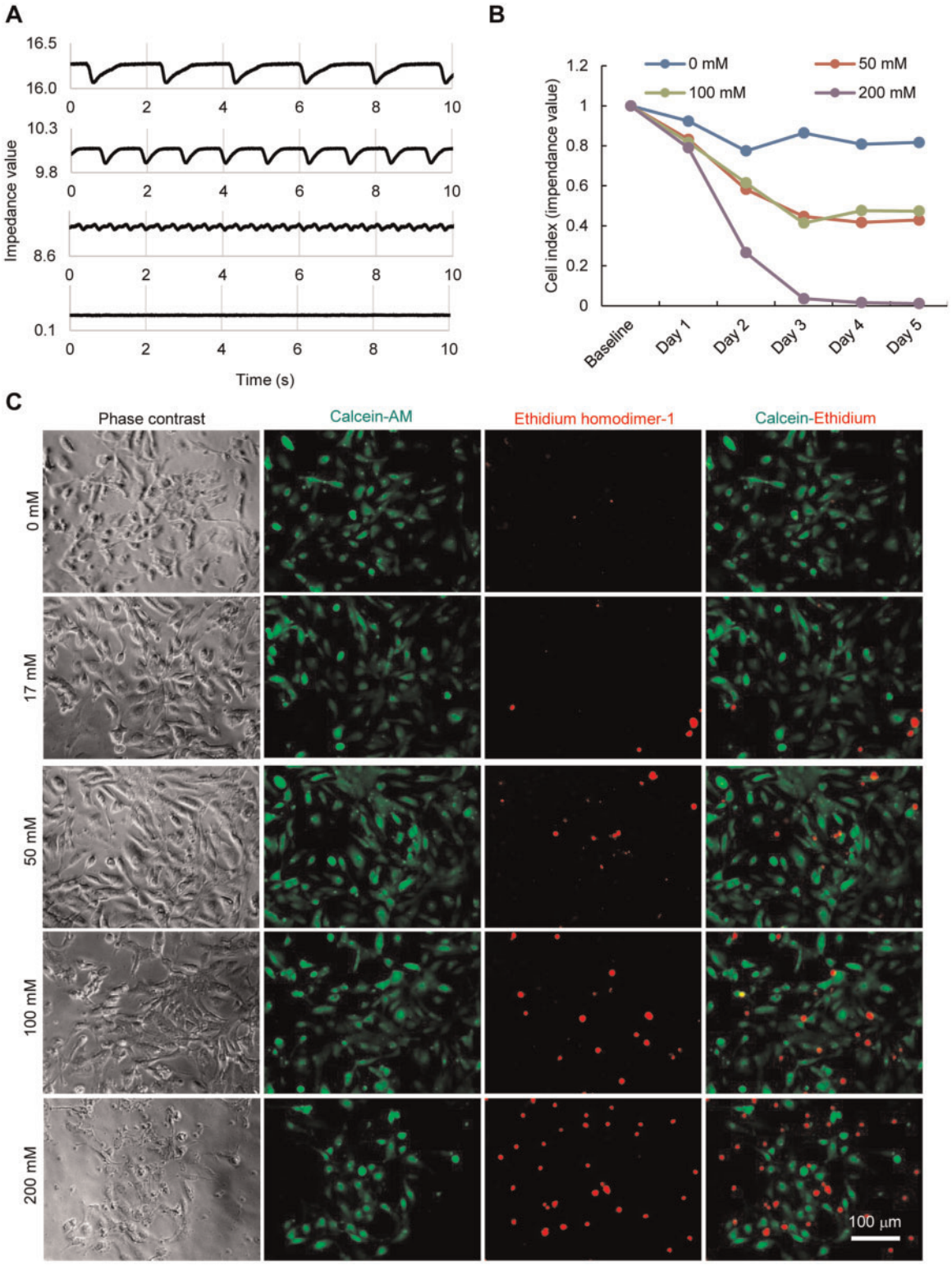

Figure 2. Ethanol exposure of hiPSC-CMs reduces cell viability and increases cytotoxicity. A, Representative trace showing cellular impedance based on xCELLigence-real-time cellular analysis. B, Graphical representation of progressive loss of cell viability upon ethanol exposure for 5 days. C, Images of LIVE/DEAD staining showing viable cells with green fluorescence from calcein AM staining and dead cells with red fluorescence from ethidium homodimer staining.

shown in Figure 2C, ethanol had dose-dependent deleterious effect on cellular viability. The cultures treated with ethanol contained more dead cells than did untreated cultures. In the culture treated with 200 mM ethanol, we observed cell detachment, and the remaining cells on the dish stopped beating and showed reduced cell viability (hence 200 mM treatment was excluded in subsequent experiments). These results were consistent with the cell index results acquired independently,

showing that ethanol induced a dose-dependent cellular damage and cell loss in hiPSC-CMs.

Ethanol Exposure Generates Cellular Oxidative Stress and Increases Production of ROS

To examine if the reduced cell viability in ethanol-treated cells was associated with increased cellular oxidative stress, we treated hiPSC-CMs with various doses of ethanol (0, 17, 50, and 100 mM ethanol) for 5 days and initially measured reactive oxygen species (ROS) by H2DCFDA probe. As shown in Figure 3A, increased ROS signals were detected in the cells treated with ethanol, suggesting exposure of ethanol induces cellular oxidative stress in hiPSC-CMs. To further confirm these results, we quantitatively measured mitochondrial ROS production through ArrayScan XTI Live High Content Platform. An algorithm software was used to detect all nuclei stained with Hoechst, and masks were generated in the area of cells stained with MitoSOX Red around the nuclei to determine the mean average fluorescence intensity of MitoSOX Red per well and the percentage of MitoSOX Red-positive cells in cultures. Treatment of hiPSC-CMs with 50 and 100 mM ethanol significantly increased mitochondrial ROS production as indicated by both mean average fluorescence intensity of MitoSOX Red and the percentage of MitoSOX Red-positive cells (Figure 3B and Supplementary Figure 2).

Effect of Ethanol Exposure on the Expression of CM-Associated Markers

To assess the effect of ethanol treatment on the expression of cardiac markers, we analyzed the expression of α-actinin and NKX2-5 in treated (17, 50, and 100 mM ethanol) and untreated hiPSC-CMs by immunocytochemical analysis. As shown in Supplementary Figure 3A, the expression of α-actinin was detected in the cytoplasm of untreated and ethanol-treated hiPSC-CMs and NKX2-5 was detected in the nuclei of α-actinin+ cells in all groups. The signal intensities of the expression of α-actinin and NKX2-5 were comparable among untreated and ethanol-treated groups, and all groups contained cells with muscle striations as detected by the expression of α-actinin (Supplementary Figure 3A). We did not observe discernable loss of sarcomeric organization in hiPSC-CMs treated with ethanol at 100 mM. In addition, we observed no significant difference among these groups in the expression of cardiac markers including α-actinin, cardiac troponin I, and cardiac troponin T as examined by qRT-PCR (Supplementary Figure 3B).

In addition, we quantitatively measured NKX2-5 expression through ArrayScan XTI Live High Content Platform. An algorithm software was used to detect all nuclei stained with Hoechst, and masks restricted to the nuclei were generated in cells stained for NKX2-5, to determine the mean average fluorescence intensity per well and the percentage of NKX2-5-positive cells in cultures. Human-induced pluripotent stem cell-derived CMs in all ethanol-treated conditions showed no significant difference in NKX2-5 expression compared with untreated cells (Supplementary Figure 4).

Ethanol Exposure Alters Intracellular Ca^{2+} Transients and Contractility in hiPSC-CMs

To test the effect of exposure of hiPSC-CMs to ethanol on Ca^{2+} handling, we assessed intracellular Ca^{2+} transients in untreated hiPSC-CMs ($n = 50$) and hiPSC-CMs treated with ethanol at 17 mM ($n = 46$) and 50 mM final concentrations ($n = 41$) using confocal line-scan imaging of cytosolic Ca^{2+}. Two categories of whole cell Ca^{2+} release events were observed: Regular Ca^{2+} transients and spontaneous Ca^{2+} waves (SCW or irregular Ca^{2+} transients). Ca^{2+} transients were categorized as "regular" if the Ca^{2+} transients recorded over 1 min had mostly consistent amplitudes and beat periods, typical cardiac transient morphology (ie, rapid upstroke and decay kinetics), and no detectable instances of spontaneous Ca^{2+} release in-between transients (eg, representative transient trace of untreated cells in Figure 4A). Ca^{2+} transients were categorized as "SCWs" (Preininger *et al.*, 2016) if they exhibited wavelets—oscillations of diastolic cytosolic Ca^{2+} in specific regions of interests along a cell, or waves—whole-cell oscillations of diastolic cytosolic Ca^{2+} (eg, representative Ca^{2+} transient traces of cells treated with 17 and 50 mM ethanol in Figure 4A). The number of cells exhibiting regular or irregular Ca^{2+} transients was counted, and percentages of the cells in each category were calculated for each condition (Figure 4B). For untreated hiPSC-CMs, the majority (83%) of the cells exhibited regular Ca^{2+} transients, with only 17% of the cells exhibiting SCWs. When the cells were treated with 17 mM ethanol, 50% of the cells had regular transients, and 50% of the cells had SCWs. When the cells were treated with 50 mM ethanol, only 22% of the cells had regular Ca^{2+} transients, and 78% of the cells had SCWs. These results suggest that exposure of hiPSC-CMs to ethanol increases the incidence of irregular Ca^{2+} transients in a dose-dependent manner. In addition, treatment of hiPSC-CMs with ROS scavenger *N*-acetyl cysteine (NAC) reduced both ethanol-induced ROS production (Supplementary Figs. 5A and B) and the incidence of abnormal Ca^{2+} transients in ethanol-treated hiPSC-CMs (Supplementary Figs. 5C and D).

We next compared cardiac contractility between untreated and ethanol-treated hiPSC-CMs using a video-based method (Huebsch *et al.*, 2015). Treatment of hiPSC-CMs with ethanol at 100 mM significantly decreased maximum contraction and maximum relaxation, although cells treated with ethanol at 17 and 50 mM did not alter these parameters (Figure 5A). Treatment of hiPSC-CMs with ethanol did not significantly alter the average of beating interval (Figure 5A). We observed, however, an increase in the incidence of irregular beating, from 15% in untreated hiPSC-CMs to 25% in cells treated with 17 and 50 mM ethanol and 30% in cells treated with 100 mM ethanol (Figure 5B). These results suggest that exposure of hiPSC-CMs to ethanol affect cardiac contractility.

RNA-seq Analysis Showed Genes Significantly Altered in hiPSC-CMs Upon Treatment With Ethanol

To further evaluate the molecular alteration of hiPSC-CMs induced by the ethanol treatment, we performed RNA-seq analysis to compare global gene expression profiles of hiPSC-CMs treated with ethanol with those without ethanol treatment. As detected by RNA-seq, 83 genes were significantly upregulated and 152 downregulated in ethanol-treated hiPSC-CMs (Figure 6A and Supplementary Figure 6). Among the top 60 genes significantly altered by ethanol exposure, 13.3% (8 genes) are members either of the potassium voltage-gated channel family or solute carrier family (Supplementary Table 4). The changes in expression of genes involved in ion channels may be in part contributing to the abnormal intracellular Ca^{2+} transients we observed in ethanol-treated hiPSC-CMs.

Gene ontology showed that ethanol upregulated the expression of genes associated with collagen metabolism and extracellular matrix (ECM) modeling in hiPSC-CMs (Figs. 6B and C). Among the top 5 upregulated genes (Supplementary Table 4), 3 were related to ECM or the reorganization of ECM (*MMP9*, *EMID1*, and *COL14A1*). Gene ontology terms also showed that most of the downregulated genes are involved in cardiovascular system development (*NPPB*, *DNAAF3*), actin filament-based process

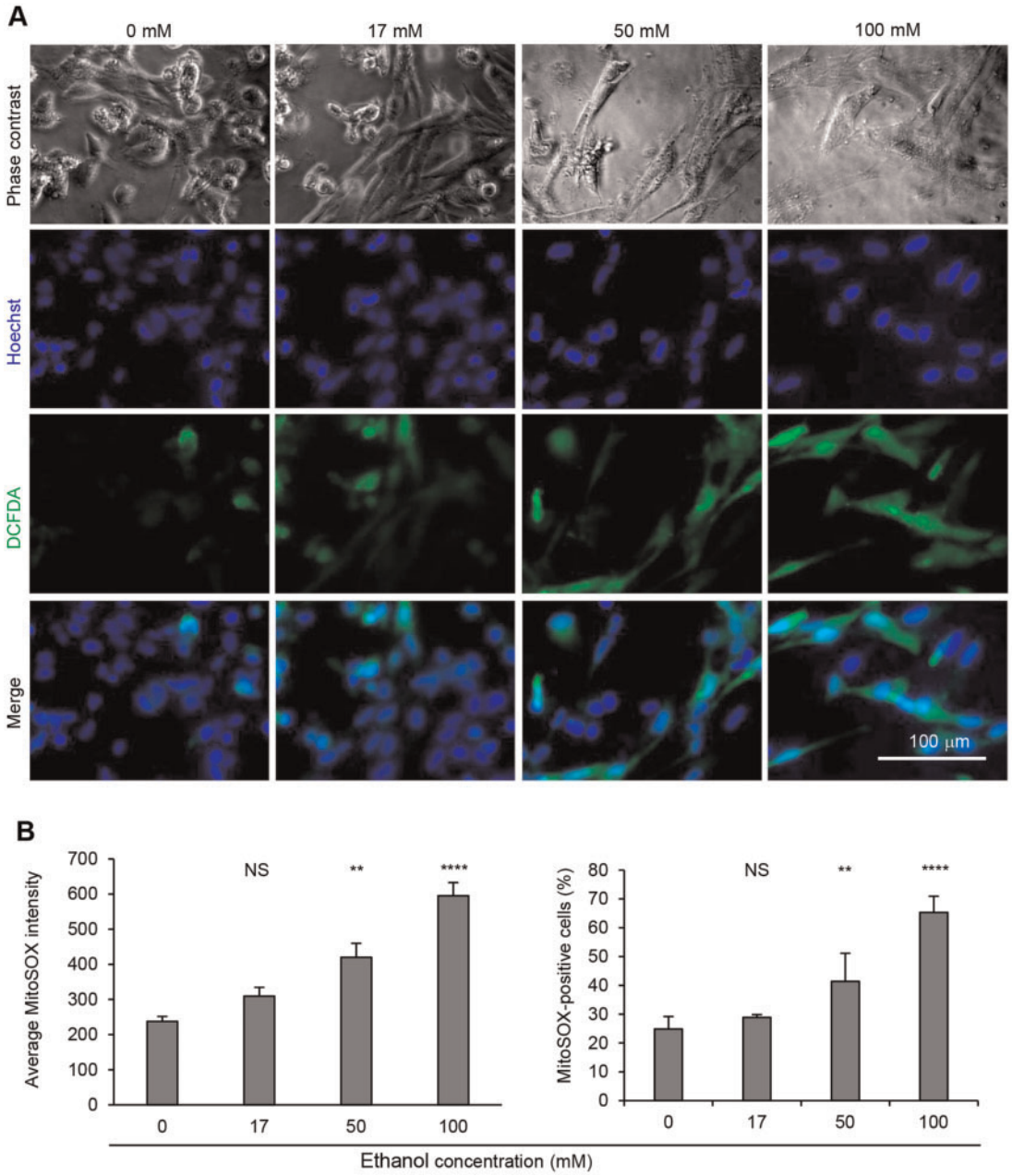

Figure 3. Ethanol exposure of hiPSC-CMs increases ROS production. A, Detection of intracellular ROS production. Human-induced pluripotent stem cell-derived cardiomyocytes were stained with DCFDA to detect ROS production upon ethanol exposure for 5 days. Reactive oxygen species-positive cells exhibited bright green cytosolic fluorescence and nuclei were stained with Hoechst. B, Detection of mitochondrial ROS production through ArrayScan. Human-induced pluripotent stem cell-derived cardiomyocytes were stained with MitoSOX Red to detect mitochondrial ROS production upon ethanol exposure for 5 days. Data presented as average fluorescence intensity per well and percentage of MitoSOX Red-positive cells, shown as mean±SD ($n = 5$). NS, no significant difference compared with control (0 mM). **p-value<.01; ****p-value < .0001. Representative images are presented in Figure S2.

(*LMOD2*, *MYH4*), and muscle contraction (*MYL2*) (Figs. 6B and C). These findings are consistent with previous studies showing a correlation between alcohol exposure and defects in heart and circulatory system development (Caputo *et al.*, 2016; Sarmah and Marrs, 2013).

DISCUSSION

Our results demonstrate that exposure of hiPSC-CMs to ethanol reduces cell viability, increases cell loss, and leads to overproduction of ROS. In functional and molecular aspects, ethanol exposure results in deranged Ca^{2+} handling in hiPSC-CMs and altered expression of genes involved in cardiovascular system development and ECM remodeling. These results indicate that hiPSC-CMs can serve as a novel, human cell-based model for the characterization of cardiac defects induced by ethanol exposure and these cells have the potential to be used as a platform for high-throughput screening and discovery of novel drugs to treat alcohol-induced cardiac defects. Furthermore, we provide a unique resource of human whole

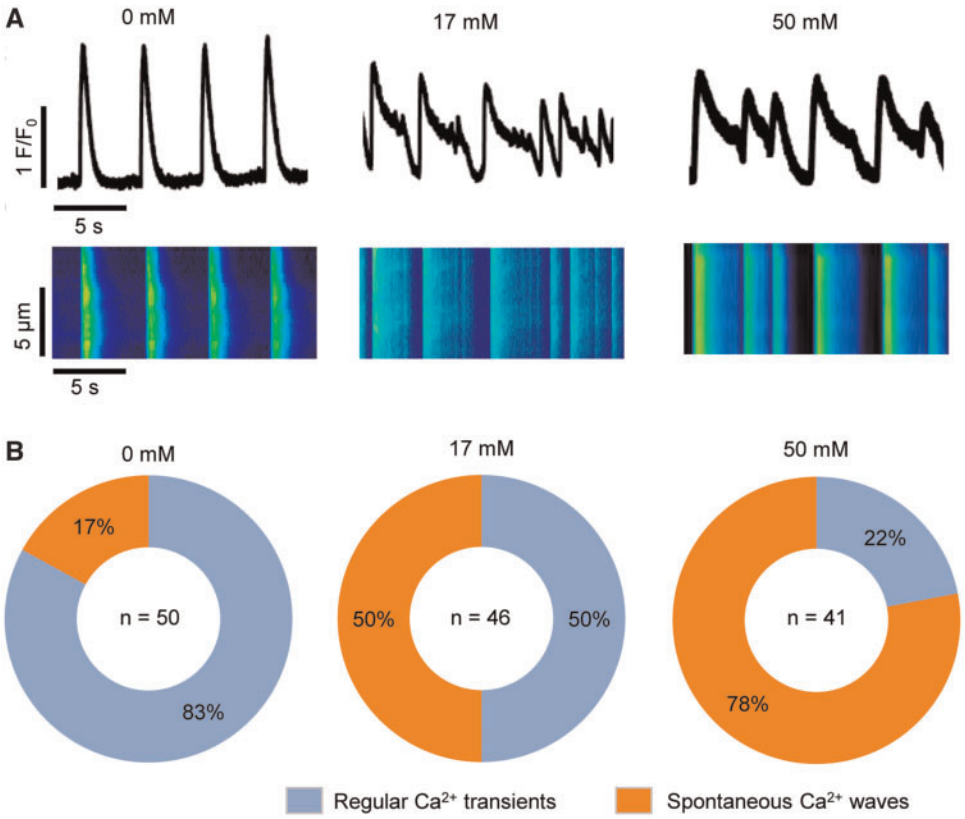

Figure 4. Ethanol exposure of hiPSC-CMs alters intracellular Ca^{2+} handling. A, Representative confocal images showing cytosolic calcium traces and line-scan of intercellular Ca^{2+} transients in cells from control (0 mM ethanol) and the treatment groups (17 and 50 mM ethanol). B, Pie chart showing the percentage of cells exhibiting regular Ca^{2+} transients or Ca^{2+} transients with spontaneous Ca^{2+} waves (SCWs) under each condition. Sample sizes (*n*) are denoted in the center of the graphs for the control and treatment groups.

transcriptomic dataset for the study of alcohol-induced cardiotoxicity (the RNA-seq data reported in this manuscript are available on the GEO database with accession number GSE125917).

Our results of ethanol-induced dose-dependent cytotoxicity, as demonstrated by ethidium homodimer staining and quantitative assessment of cell index by xCELLigence-RTCA, are consistent with previous findings in animal studies. A strong association between ethanol exposure and cellular apoptosis leading to cellular loss has been observed in various cell types including CMs (Capasso *et al.*, 1992; Chen *et al.*, 2000; Li *et al.*, 2006; Tan *et al.*, 2012). Furthermore, ethanol exposure-induced cell loss ultimately progresses to heart failure in an animal model (Capasso *et al.*, 1992).

Ethanol exposure of hiPSC-CMs also results in overproduction of ROS in a dose-dependent manner. This observation in hiPSC-CMs mirrors other animal studies that report extensive ROS generation and cell death upon ethanol exposure (Shi *et al.*, 2016; Wang *et al.*, 2015). Overproduction of ROS can lead to cellular oxidative stress which in turn results in abnormal embryogenesis (Guan *et al.*, 2004; Jing *et al.*, 2012; Kannan *et al.*, 2004; Sarmah and Marrs, 2013; Umoh *et al.*, 2014). The ROS generation has also been reported in cultured cells, including cardiac cells, upon ethanol exposure (Guan *et al.*, 2004; Jing *et al.*, 2012; Kannan *et al.*, 2004). For example, ethanol-induced ROS generation in H9c2 CMs results in apoptosis, highlighting the vital role of cellular antioxidants in attenuating ethanol-induced cytotoxicity (Shi *et al.*, 2016).

The sources of ROS generation we detected also show similarities to the observation in animal and human primary CMs upon ethanol exposure. In CMs, ROS can be generated through mitochondrial and nonmitochondrial sources (Santos *et al.*, 2011). Ethanol exposure of hiPSC-CMs results in overproduction of ROS from both mitochondrial and nonmitochondrial sources, as we detected intracellular ROS (nonmitochondrial hydrogen peroxide) with the DCFDA probe and mitochondrial ROS (mitochondrial superoxide anion) with the MitoSOX Red probe. This observation is consistent with studies showing that ethanol exposure in mice increased the production of both intracellular ROS and mitochondrial ROS in CMs (Guo and Ren, 2010; Wang *et al.*, 2015). In addition, extensive intracellular ROS production was also observed in human fetal CMs treated with ethanol or an ethanol metabolite (Li *et al.*, 2006).

Intracellular Ca^{2+} signaling plays an important role in the regulation of contraction of cardiac cells (Berridge *et al.*, 2003), and alcohol exposure increases the risk of arrhythmias (Kodama *et al.*, 2011; Mandyam *et al.*, 2012) even for individuals with modest levels of alcohol intake (Voskoboinik *et al.*, 2016). Our results show that ethanol exposure to hiPSC-CMs increases the incidence of irregular intracellular Ca^{2+} transients in the form of SCWs in a dose-dependent manner. Previous studies report intracellular Ca^{2+} dysregulation including transient irregular Ca^{2+} transients (SCWs), altered rates of decay time and rise time, or amplitude of Ca^{2+} transients, in mouse or rat CMs exposed to ethanol or its metabolite acetaldehyde (Ge *et al.*, 2011; Guo and Ren, 2010; Oba *et al.*, 2008; Zhang *et al.*, 2010). A recent study also reports that ethanol induces severe Ca^{2+} leak from sarcoplasmic reticulum (SR) in human atrial CMs and murine

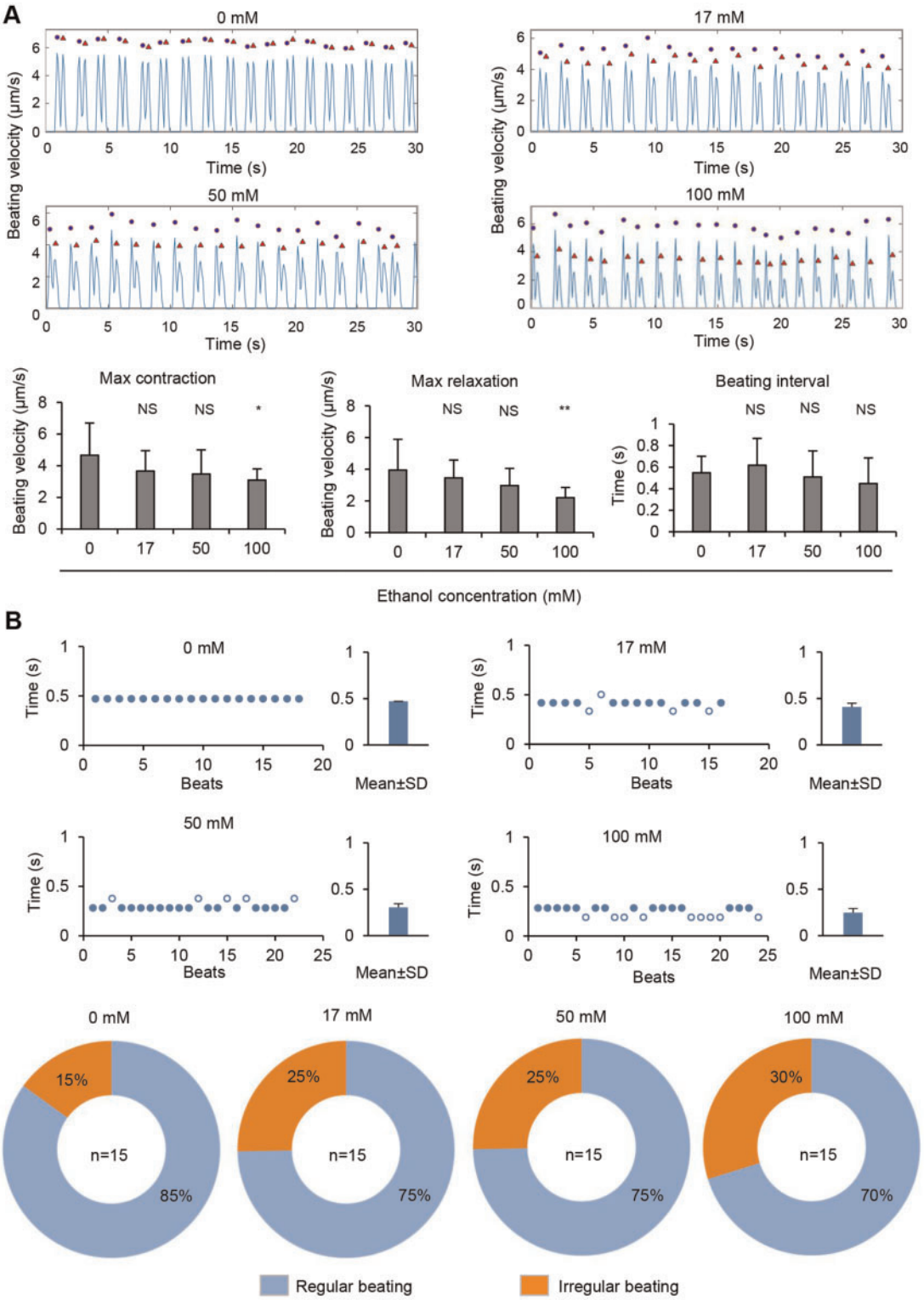

Figure 5. Ethanol exposure of hiPSC-CMs alters cells contractility. A, Video-based analysis of contractility. Representative traces show beating velocity recording of cardiomyocytes under each condition. Dots denote contraction, and triangles denote relaxation. Contraction parameters are presented as mean±SD of $n = 15$ biological samples. NS, no significant difference compared with control (0 mM). *p-value < .05; **p-value < .01. B, Scatter charts show representative traces of beating for hiPSC-CMs under each condition. The irregular beating (hollow dots) are those with beating period larger than mean+SD of beat to beat time or smaller than mean – SD of beat to beat time. Bar graphs of beating periods are presented as mean±SD of beat to beat time. Pie chart showing the percentage of cells with regular beating or irregular beating under each condition. Sample sizes (n) are denoted in the center of the graphs for the control and treatment groups.

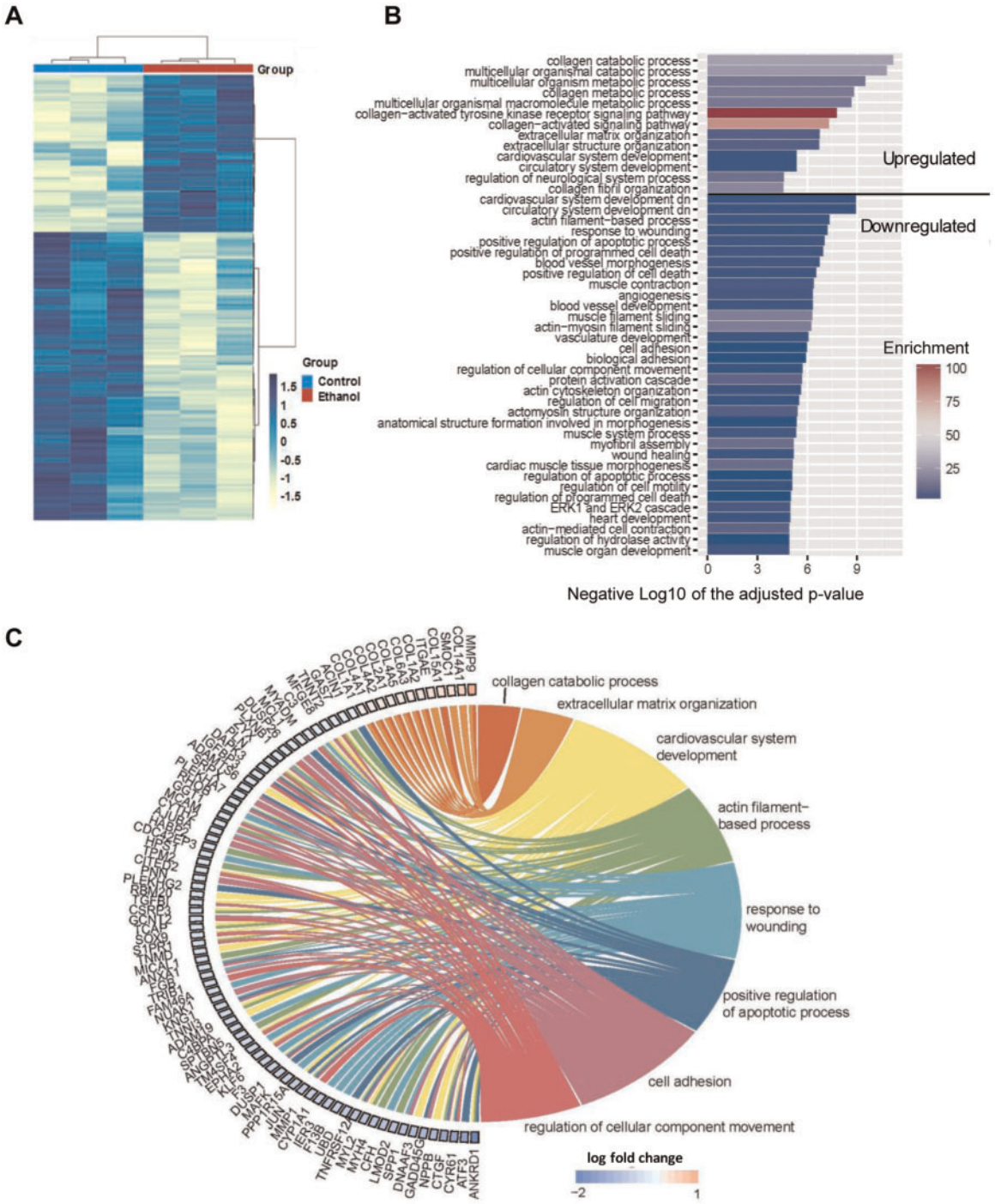

Figure 6. Differentially expressed genes and gene ontology (GO) terms identified by RNA-seq analysis of hiPSC-CMs upon treatment with ethanol. A, Heatmap of differentially expressed genes between control and ethanol-treated hiPSC-CMs ($n = 3$). B, GO results bar plot. The GO terms are summarized using REVIGO. Length of bar indicates the gene enrichment score and color of bar is –log10 (*p*-value). C, Chord diagram showing the relationship between interested GO clusters and corresponding differentially expressed genes. In each chord diagram, enriched GO terms were presented on the right, and genes contributing to these enrichments were drawn on the left. Colored squares on the left are indicated LFC value and ordered from highest to lowest LFC.

ventricular CMs (Mustroph *et al.*, 2018). Similarly, we observed persistent irregular Ca^{2+} transients indicated by oscillations of diastolic cytosolic Ca^{2+} (Ca^{2+} waves) in hiPSC-CMs. These results suggest that hiPSC-CMs can be used as a new human CM model for investigating the effect of ethanol exposure on Ca^{2+} transients and examining whether these irregular Ca^{2+} transients are responsible for ethanol-induced arrhythmogenic events.

In many cardiac disorders, deranged ion channels and Ca^{2+} signaling are linked to the overproduction of ROS (Giordano, 2005). Reactive oxygen species is known to modulate the activity of several key Ca^{2+} handling proteins, including RyR2

(cardiac ryanodine receptor) and SERCA (SR calcium transport ATPase) which are responsible for SR Ca^{2+} release and uptake, respectively (Santos *et al.*, 2011). Such modifications contribute to abnormal Ca^{2+} handling and increased risk of arrhythmia (Santos *et al.*, 2011). Consistent with the role of ROS in regulating Ca^{2+} handling, our results indicate that ROS scavenger NAC reduced the ethanol-induced ROS production and abnormal Ca^{2+} transients in hiPSC-CMs.

Our RNA-seq results reveal gene expression signatures of cardiac toxicity in hiPSC-CMs that are consistent with alcohol-induced pathophysiology observed in animal models and the clinic. For example, 3 of the top 5 upregulated genes (*MMP9*, *EMID1*, and *COL14A1*) in ethanol-treated hiPSC-CMs are related to ECM or the reorganization of ECM. Similarly, MMP9 concentrations are significantly higher in human sera of chronic alcohol abusers (Sillanaukee *et al.*, 2002), and MMP9 mRNA and protein levels are increased in the myocardium of rats following acute ethanol exposure (Li *et al.*, 2012). Collagen content in myocardium is approximately 10-fold higher in patients with alcoholic dilated cardiomyopathy than in controls without heart disease (Soufen *et al.*, 2008), and collagen mRNA and/or protein expression in the heart are significantly increased in rats following long-term exposure to alcohol (El Hajj *et al.*, 2014; Steiner *et al.*, 2015).

In summary, our results suggest that exposure of hiPSC-CMs to ethanol triggers myocyte loss, oxidative stress, and altered Ca^{2+} handling. These findings support the utility of hiPSC-CMs as a novel, physiologically relevant *in vitro* system to explore the molecular underpinnings of prenatal alcohol exposure. In addition, this cell model can be leveraged for high-throughput screening of potential drugs to treat alcohol-induced cardiac defects. For example, the irregular Ca^{2+} transients observed in ethanol-treated hiPSC-CMs may be served as a functional readout for screening antiarrhythmic drugs using high-throughput Ca^{2+} imaging. Such a study will not only advance the application of hiPSCs in drug discovery for treatment of alcohol exposure-induced heart disease but also facilitate establishment of hiPSC models for studies of alcohol-induced damages in other organs because hiPSCs have the ability to differentiate into various cell types. Moreover, hiPSC lines of variable genetic backgrounds (eg, different activities of enzymes for detoxification) may also facilitate investigation on the effects of genetic variation on the susceptibility to alcohol-induced injury as well as the development of effective treatments.

SUPPLEMENTARY DATA

Supplementary data are available at *Toxicological Sciences* online.

ACKNOWLEDGMENTS

We thank the staff at the high-throughput DNA Sequencing Core of the Parker H. Petit Institute for Bioengineering & Bioscience, Georgia Institute of Technology for their help with the preparation of the RNA-seq library.

FUNDING

Center for Pediatric Technology Center at Emory/Georgia Tech, NIH/NIEHS (P30ES019776), Woodruff Health Sciences Center, NIH/NIAAA (R21AA025723), and NIH/NHLBI (R01HL136345).

DECLARATION OF CONFILICTING INTERESTS

The authors declared no potential conflicts of interest with respect to the research, authorship, and/or publication of this article.

REFERENCES

Anders, S., and Huber, W. (2010). Differential expression analysis for sequence count data. *Genome Biol.* **11**, R106.

Anders, S., Pyl, P. T., and Huber, W. (2015). HTSeq—A Python framework to work with high-throughput sequencing data. *Bioinformatics* **31**, 166–169.

Barker, D. J., Winter, P. D., Osmond, C., Margetts, B., and Simmonds, S. J. (1989). Weight in infancy and death from ischaemic heart disease. *Lancet* **2**, 577–580.

Benjamini, Y., and Hochberg, Y. (1995). Controlling false discovery rate: A practical and powerful approach to multiple testing. *J. R. Stat. Soc. B* **57**, 289–300.

Berridge, M. J., Bootman, M. D., and Roderick, H. L. (2003). Calcium signalling: Dynamics, homeostasis and remodelling. *Nat. Rev. Mol. Cell Biol.* **4**, 517–529.

Burridge, P. W., Keller, G., Gold, J. D., and Wu, J. C. (2012). Production of de novo cardiomyocytes: Human pluripotent stem cell differentiation and direct reprogramming. *Cell Stem Cell* **10**, 16–28.

Burridge, P. W., Matsa, E., Shukla, P., Lin, Z. C., Churko, J. M., Ebert, A. D., Lan, F., Diecke, S., Huber, B., Mordwinkin, N. M., *et al.* (2014). Chemically defined generation of human cardiomyocytes. *Nat. Methods* **11**, 855–860.

Capasso, J. M., Li, P., Guideri, G., Malhotra, A., Cortese, R., and Anversa, P. (1992). Myocardial mechanical, biochemical, and structural alterations induced by chronic ethanol ingestion in rats. *Circ. Res.* **71**, 346–356.

Caputo, C., Wood, E., and Jabbour, L. (2016). Impact of fetal alcohol exposure on body systems: A systematic review. *Birth Defects Res. C Embryo Today* **108**, 174–180.

Chen, D. B., Wang, L., and Wang, P. H. (2000). Insulin-like growth factor I retards apoptotic signaling induced by ethanol in cardiomyocytes. *Life Sci.* **67**, 1683–1693.

Chen, J., Bardes, E. E., Aronow, B. J., and Jegga, A. G. (2009). ToppGene suite for gene list enrichment analysis and candidate gene prioritization. *Nucleic Acids Res.* **37**, W305–W311.

Danziger, R. S., Sakai, M., Capogrossi, M. C., Spurgeon, H. A., Hansford, R. G., and Lakatta, E. G. (1991). Ethanol acutely and reversibly suppresses excitation-contraction coupling in cardiac myocytes. *Circ. Res.* **68**, 1660–1668.

Delbridge, L. M., Connell, P. J., Harris, P. J., and Morgan, T. O. (2000). Ethanol effects on cardiomyocyte contractility. *Clin. Sci. (Lond.)* **98**, 401–407.

El Hajj, E. C., El Hajj, M. C., Voloshenyuk, T. G., Mouton, A. J., Khoutorova, E., Molina, P. E., Gilpin, N. W., and Gardner, J. D. (2014). Alcohol modulation of cardiac matrix metalloproteinases (MMPs) and tissue inhibitors of MMPs favors collagen accumulation. *Alcohol Clin. Exp. Res.* **38**, 448–456.

Fernandez-Sola, J., Preedy, V. R., Lang, C. H., Gonzalez-Reimers, E., Arno, M., Lin, J. C., Wiseman, H., Zhou, S., Emery, P. W., Nakahara, T., *et al.* (2007). Molecular and cellular events in alcohol-induced muscle disease. *Alcohol Clin. Exp. Res.* **31**, 1953–1962.

Ge, W., Guo, R., and Ren, J. (2011). AMP-dependent kinase and autophagic flux are involved in aldehyde dehydrogenase-2-induced protection against cardiac toxicity of ethanol. *Free Radic. Biol. Med.* **51**, 1736–1748.

Giordano, F. J. (2005). Oxygen, oxidative stress, hypoxia, and heart failure. *J. Clin. Invest.* **115**, 500–508.

Goh, J. M., Bensley, J. G., Kenna, K., Sozo, F., Bocking, A. D., Brien, J., Walker, D., Harding, R., and Black, M. J. (2011). Alcohol exposure during late gestation adversely affects myocardial development with implications for postnatal cardiac function. *Am. J. Physiol. Heart Circ. Physiol.* **300**, H645–H651.

Green, P. P., McKnight-Eily, L. R., Tan, C. H., Mejia, R., and Denny, C. H. (2016). Vital signs: Alcohol-exposed pregnancies–United States, 2011-2013. *MMWR Morb. Mortal Wkly. Rep.* **65**, 91–97.

Guan, Z., Lui, C. Y., Morkin, E., and Bahl, J. J. (2004). Oxidative stress and apoptosis in cardiomyocyte induced by high-dose alcohol. *J. Cardiovasc. Pharmacol.* **44**, 696–702.

Guo, R., and Ren, J. (2010). Alcohol dehydrogenase accentuates ethanol-induced myocardial dysfunction and mitochondrial damage in mice: Role of mitochondrial death pathway. *PLoS One* **5**, e8757.

Hartman, M. E., Dai, D. F., and Laflamme, M. A. (2016). Human pluripotent stem cells: Prospects and challenges as a source of cardiomyocytes for in vitro modeling and cell-based cardiac repair. *Adv. Drug Deliv. Rev.* **96**, 3–17.

Hu, C., Ge, F., Hyodo, E., Arai, K., Iwata, S., Lobdell, H. t., Walewski, J. L., Zhou, S., Clugston, R. D., Jiang, H., *et al.* (2013). Chronic ethanol consumption increases cardiomyocyte fatty acid uptake and decreases ventricular contractile function in C57BL/6J mice. *J. Mol. Cell Cardiol.* **59**, 30–40.

Huebsch, N., Loskill, P., Mandegar, M. A., Marks, N. C., Sheehan, A. S., Ma, Z., Mathur, A., Nguyen, T. N., Yoo, J. C., Judge, L. M., *et al.* (2015). Automated video-based analysis of contractility and calcium flux in human-induced pluripotent stem cell-derived cardiomyocytes cultured over different spatial scales. *Tissue Eng. Part C Methods* **21**, 467–479.

Itzhaki, I., Maizels, L., Huber, I., Zwi-Dantsis, L., Caspi, O., Winterstern, A., Feldman, O., Gepstein, A., Arbel, G., Hammerman, H., *et al.* (2011). Modelling the long QT syndrome with induced pluripotent stem cells. *Nature* **471**, 225–229.

Jha, R., Wu, Q., Singh, M., Preininger, M. K., Han, P., Ding, G., Cho, H. C., Jo, H., Maher, K. O., Wagner, M. B., *et al.* (2016). Simulated microgravity and 3D culture enhance induction, viability, proliferation and differentiation of cardiac progenitors from human pluripotent stem cells. *Sci Rep.* **6**, 30956.

Jing, L., Jin, C. M., Li, S. S., Zhang, F. M., Yuan, L., Li, W. M., Sang, Y., Li, S., and Zhou, L. J. (2012). Chronic alcohol intake-induced oxidative stress and apoptosis: Role of CYP2E1 and calpain-1 in alcoholic cardiomyopathy. *Mol. Cell Biochem.* **359**, 283–292.

Jung, C. B., Moretti, A., Mederos y Schnitzler, M., Iop, L., Storch, U., Bellin, M., Dorn, T., Ruppenthal, S., Pfeiffer, S., Goedel, A., *et al.* (2012). Dantrolene rescues arrhythmogenic RYR2 defect in a patient-specific stem cell model of catecholaminergic polymorphic ventricular tachycardia. *EMBO Mol. Med.* **4**, 180–191.

Kannan, M., Wang, L., and Kang, Y. J. (2004). Myocardial oxidative stress and toxicity induced by acute ethanol exposure in mice. *Exp. Biol. Med. (Maywood)* **229**, 553–559.

Kent, W. J., Sugnet, C. W., Furey, T. S., Roskin, K. M., Pringle, T. H., Zahler, A. M., and Haussler, D. (2002). The human genome browser at UCSC. *Genome Res.* **12**, 996–1006.

Kim, D., Langmead, B., and Salzberg, S. L. (2015). HISAT: A fast spliced aligner with low memory requirements. *Nat. Methods* **12**, 357–360.

Kodama, S., Saito, K., Tanaka, S., Horikawa, C., Saito, A., Heianza, Y., Anasako, Y., Nishigaki, Y., Yachi, Y., Iida, K. T., *et al.* (2011). Alcohol consumption and risk of atrial fibrillation: A meta-analysis. *J. Am. Coll. Cardiol.* **57**, 427–436.

Kujala, K., Paavola, J., Lahti, A., Larsson, K., Pekkanen-Mattila, M., Viitasalo, M., Lahtinen, A. M., Toivonen, L., Kontula, K., Swan, H., *et al.* (2012). Cell model of catecholaminergic polymorphic ventricular tachycardia reveals early and delayed afterdepolarizations. *PLoS One* **7**, e44660.

Kvigne, V. L., Leonardson, G. R., Neff-Smith, M., Brock, E., Borzelleca, J., and Welty, T. K. (2004). Characteristics of children who have full or incomplete fetal alcohol syndrome. *J. Pediatr.* **145**, 635–640.

Laflamme, M. A., and Murry, C. E. (2011). Heart regeneration. *Nature* **473**, 326–335.

Li, S., Korkmaz, S., Loganathan, S., Weymann, A., Radovits, T., Barnucz, E., Hirschberg, K., Hegedus, P., Zhou, Y., Tao, L., *et al.* (2012). Acute ethanol exposure increases the susceptibility of the donor hearts to ischemia/reperfusion injury after transplantation in rats. *PLoS One* **7**, e49237.

Li, S. Y., Li, Q., Shen, J. J., Dong, F., Sigmon, V. K., Liu, Y., and Ren, J. (2006). Attenuation of acetaldehyde-induced cell injury by overexpression of aldehyde dehydrogenase-2 (ALDH2) transgene in human cardiac myocytes: Role of MAP kinase signaling. *J. Mol. Cell Cardiol.* **40**, 283–294.

Lian, X., Hsiao, C., Wilson, G., Zhu, K., Hazeltine, L. B., Azarin, S. M., Raval, K. K., Zhang, J., Kamp, T. J., and Palecek, S. P. (2012). Robust cardiomyocyte differentiation from human pluripotent stem cells via temporal modulation of canonical Wnt signaling. *Proc. Natl. Acad. Sci. U.S.A.* **109**, E1848–E1857.

Love, M. I., Huber, W., and Anders, S. (2014). Moderated estimation of fold change and dispersion for RNA-seq data with DESeq2. *Genome Biol.* **15**, 550.

Mandyam, M. C., Vedantham, V., Scheinman, M. M., Tseng, Z. H., Badhwar, N., Lee, B. K., Lee, R. J., Gerstenfeld, E. P., Olgin, J. E., and Marcus, G. M. (2012). Alcohol and vagal tone as triggers for paroxysmal atrial fibrillation. *Am. J. Cardiol.* **110**, 364–368.

Mashimo, K., Arthur, P. G., and Ohno, Y. (2015). Ethanol dose- and time-dependently increases alpha and beta subunits of mitochondrial ATP synthase of cultured neonatal rat cardiomyocytes. *J. Nippon Med. Sch.* **82**, 237–245.

Mashimo, K., and Ohno, Y. (2006). Ethanol hyperpolarizes mitochondrial membrane potential and increases mitochondrial fraction in cultured mouse myocardial cells. *Arch. Toxicol.* **80**, 421–428.

Mashimo, K., Sato, S., and Ohno, Y. (2003). Chronic effects of ethanol on cultured myocardial cells: Ultrastructural and morphometric studies. *Virchows. Arch.* **442**, 356–363.

May, P. A., Gossage, J. P., Marais, A. S., Adnams, C. M., Hoyme, H. E., Jones, K. L., Robinson, L. K., Khaole, N. C., Snell, C., Kalberg, W. O., *et al.* (2007). The epidemiology of fetal alcohol syndrome and partial FAS in a South African community. *Drug Alcohol Depend.* **88**, 259–271.

Mercola, M., Colas, A., and Willems, E. (2013). Induced pluripotent stem cells in cardiovascular drug discovery. *Circ. Res.* **112**, 534–548.

Moretti, A., Bellin, M., Welling, A., Jung, C. B., Lam, J. T., Bott-Flugel, L., Dorn, T., Goedel, A., Hohnke, C., Hofmann, F., *et al.* (2010). Patient-specific induced pluripotent stem-cell models for long-QT syndrome. *N. Engl. J. Med.* **363**, 1397–1409.

Mustroph, J., Wagemann, O., Lebek, S., Tarnowski, D., Ackermann, J., Drzymalski, M., Pabel, S., Schmid, C., Wagner, S., Sossalla, S., *et al.* (2018). SR Ca(2+)-leak and disordered excitation-contraction coupling as the basis for arrhythmogenic and negative inotropic effects of acute ethanol exposure. *J. Mol. Cell Cardiol.* **116**, 81–90.

Nguyen, D. C., Hookway, T. A., Wu, Q., Jha, R., Preininger, M. K., Chen, X., Easley, C. A., Spearman, P., Deshpande, S. R., Maher, K., *et al.* (2014). Microscale generation of cardiospheres promotes robust enrichment of cardiomyocytes derived from human pluripotent stem cells. *Stem Cell Rep.* **3**, 260–268.

Oba, T., Maeno, Y., Nagao, M., Sakuma, N., and Murayama, T. (2008). Cellular redox state protects acetaldehyde-induced alteration in cardiomyocyte function by modifying Ca2+ release from sarcoplasmic reticulum. *Am. J. Physiol. Heart Circ. Physiol.* **294**, H121–H133.

Ovchinnikova, E., Hoes, M., Ustyantsev, K., Bomer, N., de Jong, T. V., van der Mei, H., Berezikov, E., and van der Meer, P. (2018). Modeling human cardiac hypertrophy in stem cell-derived cardiomyocytes. *Stem Cell Rep.*, **10**, 794–807.

Palpant, N. J., Hofsteen, P., Pabon, L., Reinecke, H., and Murry, C. E. (2015). Cardiac development in zebrafish and human embryonic stem cells is inhibited by exposure to tobacco cigarettes and e-cigarettes. *PLoS One* **10**, e0126259.

Piano, M. R., and Phillips, S. A. (2014). Alcoholic cardiomyopathy: Pathophysiologic insights. *Cardiovasc. Toxicol.* **14**, 291–308.

Polikandriotis, J. A., Rupnow, H. L., and Hart, C. M. (2005). Chronic ethanol exposure stimulates endothelial cell nitric oxide production through PI-3 kinase-and hsp90-dependent mechanisms. *Alcohol Clin. Exp. Res.* **29**, 1932–1938.

Preininger, M. K., Jha, R., Maxwell, J. T., Wu, Q., Singh, M., Wang, B., Dalal, A., McEachin, Z. T., Rossoll, W., Hales, C. M., *et al.* (2016). A human pluripotent stem cell model of catecholaminergic polymorphic ventricular tachycardia recapitulates patient-specific drug responses. *Dis. Model Mech.* **9**, 927–939.

R Development Core Team. (2014). *R: A Language and Environment for Statistical Computing*. R Foundation for Statistical Computing, Vienna, Austria.

Santos, C. X., Anilkumar, N., Zhang, M., Brewer, A. C., and Shah, A. M. (2011). Redox signaling in cardiac myocytes. *Free Radic. Biol. Med.* **50**, 777–793.

Sarmah, S., and Marrs, J. A. (2013). Complex cardiac defects after ethanol exposure during discrete cardiogenic events in zebrafish: Prevention with folic acid. *Dev. Dyn.* **242**, 1184–1201.

Savoji, H., Mohammadi, M. H., Rafatian, N., Toroghi, M. K., Wang, E. Y., Zhao, Y., Korolj, A., Ahadian, S., and Radisic, M. (2019). Cardiovascular disease models: A game changing paradigm in drug discovery and screening. *Biomaterials*, **198**, 3–26.

Shi, X., Li, Y., Hu, J., and Yu, B. (2016). Tert-butylhydroquinone attenuates the ethanol-induced apoptosis of and activates the Nrf2 antioxidant defense pathway in H9c2 cardiomyocytes. *Int. J. Mol. Med.* **38**, 123–130.

Sillanaukee, P., Kalela, A., Seppa, K., Hoyhtya, M., and Nikkari, S. T. (2002). Matrix metalloproteinase-9 is elevated in serum of alcohol abusers. *Eur. J. Clin. Invest.* **32**, 225–229.

Soufen, H. N., Salemi, V. M., Aneas, I. M., Ramires, F. J., Benicio, A. M., Benvenuti, L. A., Krieger, J. E., and Mady, C. (2008). Collagen content, but not the ratios of collagen type III/I mRNAs, differs among hypertensive, alcoholic, and idiopathic dilated cardiomyopathy. *Braz. J. Med. Biol. Res.* **41**, 1098–1104.

Steiner, J. L., Pruznak, A. M., Navaratnarajah, M., and Lang, C. H. (2015). Alcohol differentially alters extracellular matrix and adhesion molecule expression in skeletal muscle and heart. *Alcohol Clin. Exp. Res.* **39**, 1330–1340.

Sun, N., Yazawa, M., Liu, J., Han, L., Sanchez-Freire, V., Abilez, O. J., Navarrete, E. G., Hu, S., Wang, L., Lee, A., *et al.* (2012). Patient-specific induced pluripotent stem cells as a model for familial dilated cardiomyopathy. *Sci. Transl. Med.* **4**, 130ra47.

Tan, Y., Li, X., Prabhu, S. D., Brittian, K. R., Chen, Q., Yin, X., McClain, C. J., Zhou, Z., and Cai, L. (2012). Angiotensin II plays a critical role in alcohol-induced cardiac nitrative damage, cell death, remodeling, and cardiomyopathy in a protein kinase C/nicotinamide adenine dinucleotide phosphate oxidase-dependent manner. *J. Am. Coll. Cardiol.* **59**, 1477–1486.

Umoh, N. A., Walker, R. K., Al-Rubaiee, M., Jeffress, M. A., and Haddad, G. E. (2014). Acute alcohol modulates cardiac function as PI3K/Akt regulates oxidative stress. *Alcohol Clin. Exp. Res.* **38**, 1847–1864.

Voskoboinik, A., Prabhu, S., Ling, L. H., Kalman, J. M., and Kistler, P. M. (2016). Alcohol and atrial fibrillation: A sobering review. *J. Am. Coll. Cardiol.* **68**, 2567–2576.

Wang, Y., Zhao, J., Yang, W., Bi, Y., Chi, J., Tian, J., and Li, W. (2015). High-dose alcohol induces reactive oxygen species-mediated apoptosis via PKC-beta/p66Shc in mouse primary cardiomyocytes. *Biochem. Biophys. Res. Commun.* **456**, 656–661.

Watanabe, K., Ueno, M., Kamiya, D., Nishiyama, A., Matsumura, M., Wataya, T., Takahashi, J. B., Nishikawa, S., Nishikawa, S.-I., Muguruma, K., *et al.* (2007). A ROCK inhibitor permits survival of dissociated human embryonic stem cells. *Nat. Biotechnol.* **25**, 681–686.

Webster, W. S., Germain, M. A., Lipson, A., and Walsh, D. (1984). Alcohol and congenital heart defects: An experimental study in mice. *Cardiovasc. Res.* **18**, 335–338.

Worley, S. L., Vaughn, B. J., Terry, A. I., Gardiner, C. S., and DeKrey, G. K. (2015). Time- and dose-dependent effects of ethanol on mouse embryonic stem cells. *Reprod. Toxicol.* **57**, 157–164.

Xu, C. (2012). Differentiation and enrichment of cardiomyocytes from human pluripotent stem cells. *J. Mol. Cell Cardiol.* **52**, 1203–1212.

Xu, C., Inokuma, M. S., Denham, J., Golds, K., Kundu, P., Gold, J. D., and Carpenter, M. K. (2001). Feeder-free growth of undifferentiated human embryonic stem cells. *Nat. Biotechnol.* **19**, 971–974.

Yu, J., Vodyanik, M. A., Smuga-Otto, K., Antosiewicz-Bourget, J., Frane, J. L., Tian, S., Nie, J., Jonsdottir, G. A., Ruotti, V., Stewart, R., *et al.* (2007). Induced pluripotent stem cell lines derived from human somatic cells. *Science* **318**, 1917–1920.

Zhang, B., Turdi, S., Li, Q., Lopez, F. L., Eason, A. R., Anversa, P., and Ren, J. (2010). Cardiac overexpression of insulin-like growth factor 1 attenuates chronic alcohol intake-induced myocardial contractile dysfunction but not hypertrophy: Roles of Akt, mTOR, GSK3beta, and PTEN. *Free Radic. Biol. Med.* **49**, 1238–1253.